Geomechanics and Engineering, *Vol. 33, No. 4 (2023) 381-391*
https://doi.org/10.12989/gae.2023.33.4.381

Wave propagation of CNTRC beams resting on elastic foundation based on various higher-order beam theories

Yi-Wen Zhang[1], Hao-Xuan Ding[1], Gui-Lin She*[1] and Abdelouahed Tounsi[2,3,4]

[1]*College of Mechanical and Vehicle Engineering, Chongqing University, Chongqing 400044, China*
[2]*YFL (Yonsei Frontier Lab), Yonsei University, Seoul, Korea*
[3]*Department of Civil and Environmental Engineering, King Fahd University of Petroleum & Minerals, 31261 Dhahran, Eastern Province, Saudi Arabia*
[4]*Material and Hydrology Laboratory, University of Sidi Bel Abbes, Faculty of Technology, Civil Engineering Department, Algeria*

(*Received November 12, 2022, Revised March 17, 2023, Accepted March 21, 2023*)

Abstract. The aim of this work is to analyze and predict the wave propagation behavior of the carbon nanotube reinforced composites (CNTRC) beams within the framework of various higher order shear deformation beam theory. Using the Euler-Lagrange principle, the wave equations for CNTRC beams are derived, where the determining factor is to make the determinant equal to zero. Based on the eigenvalue method, the relationship between wave number and circular frequency is obtained. Furthermore, the phase and group velocities during wave propagation are obtained as a function of wave number, and the material properties of CNTRC beams are estimated by the mixture rule. In this paper, various higher order shear beam theory including Euler beam theory, Timoshenko beam theory and other beam theories are mainly adopted to analyze the wave propagation problem of the CNTRC beams, and by this way, we conduct a comparative analysis to verify the correctness of this paper. The mathematical model provided in this paper is verified numerically by comparing it with some existing results. We further investigate the effects of different enhancement modes of CNTs, volume fraction of CNTs, spring factor and other aspects on the wave propagation behaviors of the CNTRC beams.

Keywords: carbon nanotube reinforced composites; elastic foundation; various beam model; wave propagation

1. Introduction

Carbon nanotubes (CNTs) are a kind of one-dimensional quantum materials with excellent properties. CNTs have been widely used in aerospace engineering due to their high melting point, lightweight and excellent mechanical, electrical and chemical properties. It was found that the density of CNTs is only 1/6 that of steel, but the mechanical properties at tensile strength can reach 100 times than that of steel. CNTs have brought great changes to the whole industry. The excellent properties of CNTs have been investigated by many researchers (Bensattalah *et al.* 2020).

For example, Ke *et al.* (2010) studied the nonlinear free vibration of functionally graded CNTRCs beams. Rafiee *et al.* (2013) devoted to large amplitude vibration of CNTRCs beams with piezoelectric layers. Wattanasakulpong and Ungbhakorn (2013) obtained analytical solutions for bending, buckling and vibration responses of CNTRCs beams resting on elastic foundations. Hadji *et al.* (2018) performed a new quasi-3D higher shear deformation theory for vibration of CNTRCs beams supporting by elastic foundations. Shenas *et al.* (2017) elaborated the vibration of pre-twisted CNTRCs beams in thermal environment. Chen and his partners (2022) discussed the wave propagation of CNTRCs fluid-conveying pipes taking the thermal effects into consideration and using a new higher order beam theory. Zhao *et al.* (2022) performed the vibration analysis of CNTRCs double-beams incorporating thermal effects with the help of Timoshenko beam model. Civalek and his partners (2021a) presented the forced vibration analysis of CNTRCs beams using different beam models. Ebrahimi and Farazmandnia (2018) investigated the vibration characteristics of CNTRCs beams in thermal environment followed Timoshenko beam model. Considering surface effect and geometric nonlinearity, Zhang *et al.* (2021) applied the two-step perturbation method to analyze the snap-buckling behaviors of CNTRCs curved nanobeams. Tayeb *et al.* (2019) studied the scale effects on critical buckling loads of zigzag triple walled carbon nanotubes under axial compression. Timesli (2020) studied the buckling behavior of double walled carbon nanotubes using the nonlocal theory as well as Donnell shell theory. Babaei *et al.* (2021) applied the perturbation method to analyze the thermal post-buckling response of CNTRCs beams considering different boundary conditions including pinned-pinned, clamped-clamped, and clamped-roller. Babaei (2021) discussed the thermal post-buckling behaviors of CNTRCs pipes with temperature-dependent material properties. Civalek *et al.* (2021b) performed the vibration analysis of CNTRCs microbeams considering different beam models. Daikh *et al.* (2021) performed the buckling analysis of CNTRCs curved nanobeams, in which the thermal effects are taken into account. Esen *et al.* (2022) discussed the vibration response of CNTRCs nanobeams

*Corresponding author, Associate Professor
E-mail: sheguilin@cqu.edu.cn

ISSN: 2005-307X (Print), 2092-6219 (Online)

subjected to moving point loadings based on nonlocal strain gradient theory. Peng *et al.* (2022) revealed the free vibration characteristics of CNTRCs beams with initial geometric imperfection using the first-order shear theory. Karamanli and Vo (2021) proposed a finite element model for the analysis of CNTRCs beams, in which the shear deformation is included. Sekmi (2021) paid attention to the nonlinear vibration vibration of clamped-clamped buckled CNTRCs beams, in which the pre-and post-buckling states are considered. Talebizadehsardari *et al.* (2020) studied the static bending of CNTRCs curved beams, in which the simply supported ends are considered. In addition, as a novel composite material, functionally graded materials have also attracted researchers' interest (Malikan and Eremeyev 2021, Barretta *et al.* 2020, Golmakani *et al.* 2021, Heydari *et al.* 2018, Zenkour 2018, Zenkour and Radwan 2019, Zouatnia *et al.* 2017, Xu *et al.* 2022). Although relevant scholars have conducted extensive research in relevant fields over the past few years (e.g., Alazwari *et al.* 2021, Assie *et al.* 2023, Babaei 2022a, b, Babaei and Eslami 2021a, b, Basha *et al.* 2022, Faghidian and Elishakoff 2022a, b, Faghidian *et al.* 2022c, Faghidian *et al.* 2023a, b, c, Hendi *et al.* 2022, Mohamed *et al.* 2021, 2019, Melaibari *et al.* 2023, Chen *et al.* 2022a, b, Ding and She 2021, 2023, Ding *et al.* 2022a, b, Gan and She 2023, Gan *et al.* 2023, Li *et al.* 2023, Lu *et al.* 2021, She 2020, 2021, She and Ding 2023, She *et al.* 2018, 2021, 2022, She and Li 2022, Xu and She 2022, Zhang *et al.* 2022, 2023a, b, c, Zhang and She 2022, 2023a, b, Zhang *et al.* 2021, Zhao *et al.* 2022a, b), the topic of this article has not yet been studied by scholars. Especially, there is no papers studying the wave propagation of CNTRC beams resting on elastic foundations.

Through literature searching, it can be found that the existing researches on the CNTRC beams only studied the bending wave, but did not study the longitudinal wave and shear wave. Because of the existence of various forms of waves in the structure, it would be unreasonable to ignore the propagation of other waves, so it is necessary to carry out the study of longitudinal wave and shear wave. In addition, most of the published literature uses Timoshenko and Euler-Bernoulli beam theory to establish the model. To the author's knowledge, no one has used various high-order shear deformation beam theory to study the wave propagation in CNTRC beams. Therefore, this problem remains to be solved.

This paper has the following three innovations:

i) The wave propagation model of CNTRCs beams is established by using the various beam models, and three different distribution types of CNTs are considered;

ii) We study the phase velocity and group velocity of longitudinal, flexural and shear waves in CNTRCs beams.

iii) We studied the influence of different volume fractions, elastic coefficients on the wave propagation behaviors of CNTRCs beams.

2. CNTRCs beams

In this paper, we consider a straight CNTRCs beam with the height h and length L, which is made from the isotropic polymer matrix and CNTs. This beam rests on elastic foundations incorporating shear layers k_s and Winkler springs k_w, see Fig. 1. In addition, depicted in Fig. 1 is the three CNTs reinforcement patterns. The expressions for estimating the effective Young's modulus and shear modulus of CNTRC beams have the following forms (Civalek *et al*. 2021, Ebrahimi and Rostami 2018)

$$E_{11}=\eta_1 V_{cnt}E_{11}^{cnt}+\left(1\text{-}V_{cnt}\right)E^{p}$$

$$\frac{\eta_3}{G_{12}}=\frac{V_{cnt}}{G_{12}^{cnt}}+\frac{\left(1\text{-}V_{cnt}\right)}{G^{p}} \tag{1}$$

with $[E_{11}^{cnt}, G_{12}^{cnt}]$ being [Young's; shear] modulus, $[E^p, G^p]$ being [Young's; shear] modulus of the polymer matrix, $V_{cnt}$is the volume fractions of the CNTs. Considering the scale-dependent material properties, the CNTs efficiency parameter η_i (i=1,2,3) is introduced, and the elastic modulus of CNTRC beams obtained by MD simulation is matched with the numerical results obtained by mixing law to determine its value. By using the same rules, the Poisson's ratio (v) and the mass density (ρ) of the CNTRCs beams can been written as (Civalek *et al*. 2021, Ebrahimi and Rostami 2018)

$$v=V_{cnt}v^{cnt}+\left(1\text{-}V_{cnt}\right)v^{p}$$

$$\rho=V_{cnt}\rho^{cnt}+\left(1\text{-}V_{cnt}\right)\rho^{p} \tag{2}$$

with $[v^{cnt},\rho^{cnt}]$ being [Poisson's ratio; mass density] of the CNTs, $[v^p, \rho^p]$ being [Poisson's ratio; mass density] of the polymer matrix, $[E^p, G^p]$being[Young's; shear] modulus of the polymer matrix. The different CNTs reinforcement patterns are also shown in Fig. 2, the continuous functions of CNTs volume fraction for different distributions are as follows (Civalek *et al*. 2021, Ebrahimi and Rostami 2018)

$$V_{cnt}=\begin{cases} V_{cnt}^{*} & \text{for UD case} \\ 2(1-2\dfrac{|z|}{h})V_{cnt}^{*} & \text{for O case} \\ 4\dfrac{|z|}{h}V_{cnt}^{*} & \text{for X case} \end{cases} \tag{3}$$

Herein, V_{cnt}^{*} is the volume fraction of the given CNTs, which is calculated as

$$V_{cnt}^{*}=\frac{W_{cnt}}{W_{cnt}+(\rho^{cnt}/\rho^{m})(1-W_{cnt})} \tag{4}$$

During the calculation, the CNTs efficiency parameters and the given volume fraction (V_{CNT}^{*}) are: η_1 =1.2833 and η_2 = η_3 =1.0556 when V_{CNT}^{*} =0.12; η_1 =1.3414 and η_2 = η_3 =1.7101 when V_{CNT}^{*} =0.17; η_1 =1.3238 and η_2 = η_3=1.7380when V_{CNT}^{*}=0.28 (Civalek *et al.* 2021, Ebrahimi and Rostami 2018).

3.Wave equations

Using the higher-order shear deformation theory, the

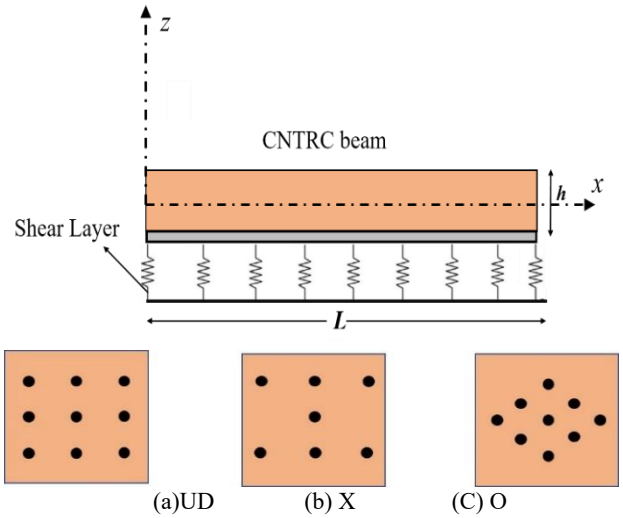

Fig. 1 Geometric dimensions of CNTRC beam and distribution pattern of CNTs in the cross-section

displacement field components of the CNTRC beam are assumed to be (Wattanasakulpong and Ungbhakorn 2013, She *et al*. 2018)

$$\begin{aligned} u(x,z,t) &= u_0 - z\frac{\partial w_0(x,t)}{\partial x} + \Psi(z)\, f_0(x,t) \\ v(x,y,z,t) &= 0 \\ w(x,z,t) &= w_0(x,t) \end{aligned} \tag{5}$$

where the displacement in the y-axis direction is 0, u_0 and $w_0(x,t)$ denote the displacements of the point in the x- and z- directions in the reference plane, respectively, t denotes time, and $f_0(x,t)$ have the following form

$$f_0(x,t) = \frac{\partial w_0(x,t)}{\partial x} - \phi_0(x,t) \tag{6}$$

where $\phi_0(x,t)$ is rotation, the purpose of the shape function (Ψ) in the Eq. (5(a)) is to describe the distribution of transverse shear stresses in the thickness direction of the transverse beams. The shape function (Ψ) vary with different beam theories (Wattanasakulpong and Ungbhakorn 2013)

$$\Psi(z) = \begin{cases} 0 & \text{Euler beam model} \\ z & \text{Timoshenko-Ehrenfest model} \\ z(1-\frac{4z^2}{3h^2}) & \text{Reddy beam model} \\ \frac{h}{\pi}\sin(\frac{\pi z}{h}) & \text{Trigonometric beam model} \\ ze^{-2(z/h)^2} & \text{Exponential beam model} \\ h\sinh(\frac{z}{h}) - z\cosh(\frac{1}{2}) & \text{Hyperbolic beam model} \end{cases} \tag{7}$$

Because Reddy beam model does not require the introduction of shear factors, it has been widely used, So, in this study, the Reddy beam model is adopted to build the model. The axial and shear strains can be expressed as follows (Wattanasakulpong and Ungbhakorn 2013, She *et al*. 2018)

$$\begin{aligned} \varepsilon_{xx} &= \frac{\partial u}{\partial x} = \frac{\partial u_0}{\partial x} - z\frac{\partial^2 w_0}{\partial x^2} + \Psi(z)(\frac{\partial^2 w_0}{\partial x^2} - \frac{\partial \phi_0}{\partial x}) \\ \gamma_{xz} &= \frac{\partial u}{\partial z} + \frac{\partial w}{\partial x} = \frac{\partial \Psi(z)}{\partial z}(\frac{\partial w_0}{\partial x} - \phi_0) \end{aligned} \tag{8}$$

Next, the Euler-Lagrange principle is employed to derive the wave equations. The total energy mainly comes from two parts, one is strain energy U_b and elastic potential energy U_f, the other is kinetic energy K.

The strain energy U_b and elastic potential energy U_f have the following expressions (Wattanasakulpong and Ungbhakorn 2013)

$$\begin{aligned} U_b &= \frac{1}{2}\int_V (\sigma_x \varepsilon_{xx} + \sigma_{xz}\gamma_{xz})dV \\ &= \frac{1}{2}\int_0^L \left[N_x \frac{\partial u_0}{\partial x} + P_x(\frac{\partial^2 w_0}{\partial x^2} - \frac{\partial \phi_0}{\partial x}) + Q_x(\frac{\partial w_0}{\partial x} - \phi_0) \right] dX \\ U_f &= \frac{1}{2}\int_0^L \left[k_w w_0^2 + k_s(\frac{\partial w}{\partial x})^2 \right] dX \end{aligned} \tag{9}$$

$$\begin{aligned} [N_x, M_x, P_x] &= \int_A \sigma_{xx}[1, z, \Psi(z)]dA \\ Q_x &= \int_A \frac{d\Psi(z)}{dz}\sigma_x dA \end{aligned} \tag{10}$$

The kinetic energy has the following expression (Wattanasakulpong and Ungbhakorn 2013, She *et al*. 2018)

$$\begin{aligned} K &= \frac{1}{2}\int_V \left[\rho(\frac{\partial u}{\partial t})^2 + \rho(\frac{\partial w}{\partial t})^2 \right] dV \\ &= \frac{1}{2}\int_0^L \int_A \rho(z) \begin{bmatrix} (\frac{\partial u_0}{\partial t})^2 + (\frac{\partial w_0}{\partial t})^2 + z^2(\frac{\partial^2 w_0}{\partial x \partial t})^2 \\ +\Psi(z)^2(\frac{\partial^2 w_0}{\partial x \partial t} - \frac{\partial \phi_0}{\partial t})^2 \\ -2z\frac{\partial u_0}{\partial t}\frac{\partial^2 w_0}{\partial x \partial t} \\ +2\Psi(z)\frac{\partial u_0}{\partial t}(\frac{\partial^2 w_0}{\partial x \partial t} - \frac{\partial \phi_0}{\partial t}) \\ -2z\Psi(z)\frac{\partial^2 w_0}{\partial x \partial t}(\frac{\partial^2 w_0}{\partial x \partial t} - \frac{\partial \phi_0}{\partial t}) \end{bmatrix} dA dX \\ &= \frac{1}{2}\int_0^L \begin{bmatrix} I_0\left[(\frac{\partial u_0}{\partial t})^2 + (\frac{\partial w_0}{\partial t})^2 \right] + I_2(\frac{\partial^2 w_0}{\partial x \partial t})^2 \\ +I_5\left[(\frac{\partial^2 w_0}{\partial x \partial t})^2 - 2\frac{\partial u_0}{\partial t}\frac{\partial^2 w_0}{\partial x \partial t} + (\frac{\partial \phi_0}{\partial t})^2 \right] \\ -2I_1\frac{\partial u_0}{\partial t}\frac{\partial^2 w_0}{\partial x \partial t} \\ +2I_3\left[2\frac{\partial^2 w_0}{\partial x \partial t}\frac{\partial u_0}{\partial t} - 2\frac{\partial u_0}{\partial t}\frac{\partial \phi_0}{\partial t} \right] \\ +I_4\left[2\frac{\partial^2 w_0}{\partial x \partial t}\frac{\partial \phi_0}{\partial t} - 2(\frac{\partial^2 w_0}{\partial x \partial t})^2 \right] \end{bmatrix} dX \end{aligned} \tag{11}$$

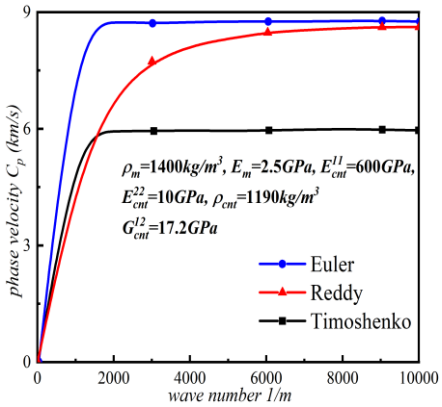

Fig. 2 Comparative analysis

Herein (Wattanasakulpong and Ungbhakorn 2013)

$$[I_0, I_1, I_2] = \int_A \rho(z)[1, z, z^2]dA$$
$$[I_3, I_4] = \int_A \Psi(z)\rho(z)[1, z]dA \quad (12)$$
$$[I_5] = \int_A \Psi^2(z)\rho(z)dA$$

Applying the Euler-Lagrangian method to derived the motion equation, then we have (Wattanasakulpong and Ungbhakorn 2013)

$$\frac{\partial N_x}{\partial x} = I_0\ddot{u}_0 - I_1\frac{\partial\ddot{\omega}_0}{\partial x} + I_3(\frac{\partial\ddot{\omega}_0}{\partial x} - \ddot{\phi}_0), \quad (13)$$

$$\frac{\partial P_x}{\partial x} - Q_x = I_3\ddot{u}_0 - I_4\frac{\partial\ddot{\omega}_0}{\partial x} + I_5(\frac{\partial\ddot{\omega}_0}{\partial x} - \ddot{\phi}_0), \quad (14)$$

$$\frac{\partial^2 P_x}{\partial x^2} - \frac{\partial^2 M_x}{\partial x^2} - \frac{\partial Q_x}{\partial x} + K_w\omega_0 - K_s\frac{\partial^2\omega_0}{\partial x^2}$$
$$-q + N_T\frac{\partial^2\omega_0}{\partial x^2} = -I_0\ddot{\omega}_0 - I_1\frac{\partial\ddot{u}_0}{\partial x} + I_2\frac{\partial^2\ddot{\omega}_0}{\partial x^2} \quad (15)$$
$$+I_3\frac{\partial\ddot{u}_0}{\partial x} + I_4(\frac{\partial\ddot{\phi}_0}{\partial x} - 2\frac{\partial^2\ddot{\omega}_0}{\partial x^2}) + I_5(\frac{\partial^2\ddot{\omega}_0}{\partial x^2} - \frac{\partial\ddot{\phi}_0}{\partial x}).$$

In addition, the normal stresses, shear stresses, axial and generalized forces and shear forces can be expressed as

$$\begin{bmatrix}\sigma_{xx}\\ \tau_{xz}\\ Q_{11}(z)\\ Q_{55}(z)\end{bmatrix} = \begin{bmatrix}Q_{11}(z)\varepsilon_{xx}\\ Q_{55}(z)\gamma_{xz}\\ E_{11}(z)\\ G_{12}(z)\end{bmatrix}$$

$$\begin{bmatrix}N_x\\ M_x\\ P_x\\ Q_x\end{bmatrix} = \begin{bmatrix}A_{11} & -B_{11} & C_{11}\\ B_{11} & -D_{11} & E_{11}\\ C_{11} & -E_{11} & H_{11}\\ 0 & 0 & A_{11}\end{bmatrix}\begin{bmatrix}\frac{\partial u_0}{\partial x}\\ \frac{\partial^2\omega_0}{\partial x^2}\\ \frac{\partial^2\omega_0}{\partial x^2} - \frac{\partial\phi_0}{\partial x}\end{bmatrix} \quad (16)$$

In which (Wattanasakulpong and Ungbhakorn 2013)

$$[A_{11}, B_{11}, D_{11}] = \int_A Q_{11}[1, z, z^2]dA$$
$$[C_{11}, E_{11}] = \int_A Q_{11}\Psi_{(z)}[1, z]dA \quad (17)$$
$$H_{11} = \int_A Q_{11}\Psi^2_{(z)}dA,\ A_{55} = \int_A Q_{55}(\frac{\partial\Psi_{(z)}}{\partial z})^2 dA$$

For Timoshenko–Ehrenfest beam, $A_{55} = \int_A \frac{5}{6}Q_{55}(\frac{\partial\Psi_{(z)}}{\partial z})^2 dA$ .The substitution Eq. (15) into Eq. (14) leads to following wave equations

$$A_{11}\frac{\partial^2 u_0}{\partial x^2} - B_{11}\frac{\partial^3\omega_0}{\partial x^3} + C_{11}(\frac{\partial^3\omega_0}{\partial x^3} - \frac{\partial^2\phi_0}{\partial x^2})$$
$$= I_0\ddot{u}_0 - I_1\frac{\partial\ddot{\omega}_0}{\partial x} + I_3(\frac{\partial\ddot{\omega}_0}{\partial x} - \ddot{\phi}_0),$$
$$C_{11}\frac{\partial^2 u_0}{\partial x^2} - E_{11}\frac{\partial^3\omega_0}{\partial x^3} + H_{11}(\frac{\partial^3\omega_0}{\partial x^3} - \frac{\partial^2\phi_0}{\partial x^2})$$
$$-A_{55}(\frac{\partial\omega_0}{\partial x} - \phi_0) = I_3\ddot{u}_0 - I_4\frac{\partial\ddot{\omega}_0}{\partial x} + I_5(\frac{\partial\ddot{\omega}_0}{\partial x} - \ddot{\phi}_0),$$
$$C_{11}\frac{\partial^3 u_0}{\partial x^3} - E_{11}\frac{\partial^4\omega_0}{\partial x^4} + H_{11}(\frac{\partial^4\omega_0}{\partial x^4} - \frac{\partial^3\phi_0}{\partial x^3}) \quad (18)$$
$$-B_{11}\frac{\partial^3 u_0}{\partial x^3} + D_{11}\frac{\partial^4\omega_0}{\partial x^4} - E_{11}(\frac{\partial^4\omega_0}{\partial x^4} - \frac{\partial^3\phi_0}{\partial x^3})$$
$$-A_{55}(\frac{\partial^2\omega_0}{\partial x^2} - \frac{\partial\phi_0}{\partial x}) + K_\omega\omega_0 - K_s\frac{\partial^2\omega_0}{\partial x^2} - q$$
$$-N_{x0}\frac{\partial^2\omega_0}{\partial x^2} = -I_0\ddot{\omega}_0 - I_1\frac{\partial\ddot{u}_0}{\partial x} + I_2\frac{\partial^2\ddot{\omega}_0}{\partial x^2} + I_3\frac{\partial\ddot{u}_0}{\partial x}$$
$$+I_4(\frac{\partial\ddot{\phi}_0}{\partial x} - 2\frac{\partial^2\ddot{\omega}_0}{\partial x^2}) + I_5(\frac{\partial^2\ddot{\omega}_0}{\partial x^2} - \frac{\partial\ddot{\phi}_0}{\partial x}).$$

4. Analytical solutions

The wave equations in Eq. (18) can be solved analytically. We assume that the solutions for free boundary conditions are shown as follows (She *et al*. 2018)

$$U_0(x,t) = U_m e^{i(kx-\omega t)}$$
$$\Phi_0(x,t) = \Phi_m e^{i(kx-\omega t)} \quad (19)$$
$$W_0(x,t) = W_m e^{i(kx-\omega t)}$$
$$i = \sqrt{-1} \quad (20)$$

with [w , k] being [circular frequency; wave number], U_m, Ψ_m, and W_m are the coefficients of the wave frequency.

Substituting Eqs. (19(a))-(19(c)) into the equations of Eqs. (18(a))-(18(c)), then we have

$$\begin{bmatrix}a_{11} & a_{12} & a_{13}\\ a_{21} & a_{22} & a_{23}\\ a_{31} & a_{32} & a_{33}\end{bmatrix}\begin{Bmatrix}U_m\\ \Phi_m\\ W_m\end{Bmatrix} = \begin{Bmatrix}0\\ 0\\ q\end{Bmatrix} \quad (21)$$

In which

$$\begin{aligned}
a_{11} &= I_0\omega^2 - k^2 A_{11} \\
a_{12} &= C_{11}k^2 - I_3\omega^2 \\
a_{13} &= B_{11}ik^3 - C_{11}ik^3 - I_1 ik\omega^2 + I_3 ik\omega^2 \\
a_{21} &= -k^2 C_{11} + I_3\omega^2 \\
a_{22} &= H_{11}k^2 + A_{55} - I_5\omega^2 \\
a_{23} &= E_{11}ik^3 - ik^3 H_{11} - A_{55}ik + ik\omega^2 I_4 + I_5 ik\omega^2 \quad (22) \\
a_{31} &= -C_{11}ik^3 + B_{11}ik^3 - I_1 ik\omega^2 + I_3 ik\omega^2 \\
a_{32} &= H_{11}ik^3 - E_{11}ik^3 + A_{55}ik - ik\omega^2 I_4 - I_5 ik\omega^2 \\
a_{33} &= -E_{11}k^4 + H_{11}k^4 + D_{11}k^4 - E_{11}k^4 \\
&+ A_{55}k^2 + K_w + K_s k^2 - N_{xo}k^2 - I_0\omega^2 \\
&- I_2 k^2\omega^2 + 2k^2\omega^2 - I_5 k^2\omega^2
\end{aligned}$$

Then we set the coefficient matrix equal to 0, so that we can obtain an expression for the relationship between the wave number and the circular frequency, and thus deriving an expression for the phase velocity and group velocity of the longitudinal, shear and bending waves.

5. Numerical analyses and calculation

In the following study, the calculated data are as follows (Wattanasakulpong and Ungbhakorn 2013):$\upsilon^p = 0.3$;$\rho^p = 1190kg/m^3$and $E^p = 2.5GPa$. For reinforcement material, the material properties of CNTs are: $\upsilon^{cnt} = 0.19$; $\rho^{cnt} = 1400kg/m^3$; $E_{11}^{cnt} = 600GPa$; $E_{22}^{cnt} = 10GPa$ and $G_{12}^{cnt} = 17.2GPa$.

Fig. 2 shows the phase velocity-wave number diagram of UD-Beam bending waves under different Euler, Reddy and Timoshenko beam theories. The phase velocity calculated by Euler and Timoshenko beams is the most intense with the increase of wave number when the beam number is small. With the gradual increase of wave number, the phase velocity tends to be stable and converges to a certain value, in which the Euler beam theory phase velocity is the largest, the Reddy beam theory phase velocity is the second, and the Timoshenko beam theory phase velocity is the smallest. The Timoshenko beam theory is minimal.

Figs. 3-5 illustrate the relationship between longitudinal, shear and bending wave phase velocities versus wave number for UD, X and V beams at different volume fractions of CNTs. (Where the UD, X and V beams are the result of different arrangements and distributions of CNTs on the polymer matrix). As we can see from the pictures (c) of these three figures, the longitudinal waves along the X-axis are constant for the three reinforcement types of beams during wave propagation and do not vary with the wave number. Since all the three types of CNTRC beams are symmetrically distributed, the values of the longitudinal waves are the same for all three types of beams with the same volume fraction of CNTs, and increase in parallel as the volume fraction of CNTs increases. In the process of wave propagation, the displacement of the three reinforced beams along the X-axis is constant and does not change with the wave number. Although the distribution patterns of CNTs on the polymer matrix are different, because the three types of beams are symmetrically distributed, the longitudinal wave values are the same for the three types of beams with the same CNTs volume fraction, and the longitudinal wave values increase in parallel with the increase of the CNTs volume fraction.

In picture (b) of Figs. 3-5, the phase velocity of shear waves due to torsion is given as a function of wave number for three different CNTRC beams with different values of CNTs volume fraction. The images show that for the same volume fraction of CNTs, the phase velocity of shear waves tends to decrease with the increase of wave number. Whereas the phase velocity decreases sharply when the value of wave number is small (k less than 2000 (1/m)), as the wave number continues to increase, the phase velocity tends to level off and keeps approaching the value of 8 (km/s). Secondly, the graphs also show that the phase velocity of the CNTRC beams decreases with increasing volume fraction of CNTs for the same wave number.

For the case of bending waves, in picture (a) of Figs. 3-5, according to different volume fraction of CNTs, the relationship between bending wave and wave number caused by volume bending of three different CNTRC beams is given. The images show that in contrast to the trend of shear wave, the phase velocity of the bending waves tends to increase as the wave number increased for the same volume fraction of CNTs. And when the value of wave number is small (less than 2000 (1/m)), the phase velocity increases sharply. It is further observed that when the wave number is small, an increase in wave number has the greatest effect on the phase velocity of the X-beam, followed by the UD-beam, with the O-beam having the least effect. As the wave number continues to increase, the phase velocity tends to level off and keeps approaching the value of 8 (km/s). Secondly, the graph also shows that the beam with more CNTs has a higher phase velocity when the wave number is the same. Comparing the bending waves of these three different types of beams, we can see that the phase velocity is greatest for UD beams and least for X beams for the same number of waves when the volume fraction of CNTs is 0.12, with the same pattern for $V_{cnt}^* = 0.17$ and $V_{cnt}^* = 0.28$..

Figs. 6-8 illustrate the effect of the volume fraction of CNTs on the group velocities of longitudinal, shear and bending waves in the UD, X and O-beams during wave propagation, respectively. As can be seen in picture (c) of these three figures, in the same direction as the longitudinal phase velocity, the longitudinal group velocity along the X-axis is constant for all three types of beams, and for the same CNT volume fraction, the longitudinal group velocity is the same, also for the same wave number k, it increases with the increase of the CNT volume percentage. Picture (b) of Figs. 6-8 demonstrates the effect of wave number as well as CNTs volume fraction on the shear wave group velocity of a CNTRC beams during wave propagation, we can clearly see that regardless of the symmetrical pattern in which the CNTs are distributed on the polymer matrix, the

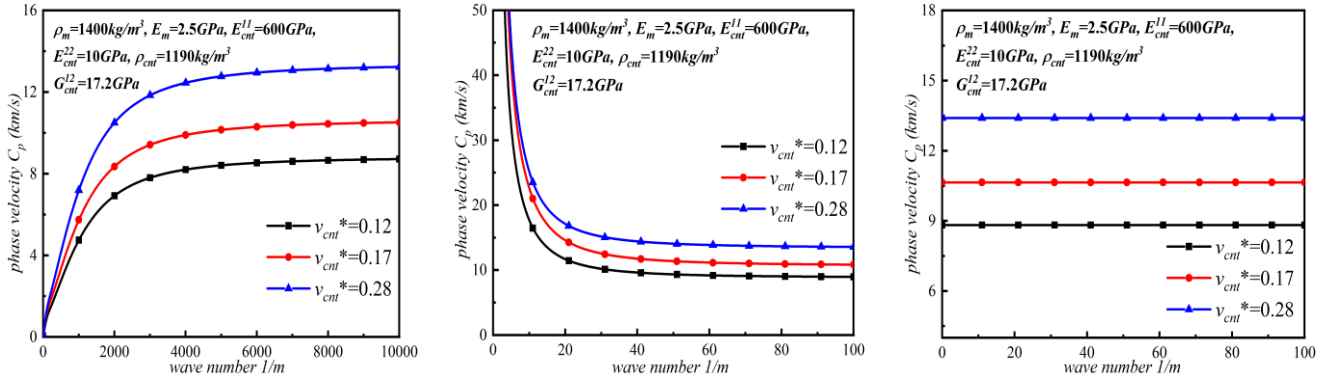

(a) (b) (c)

Fig. 3 Wave propagation diagram with different volume fractions of CNTs (UD-Beam)

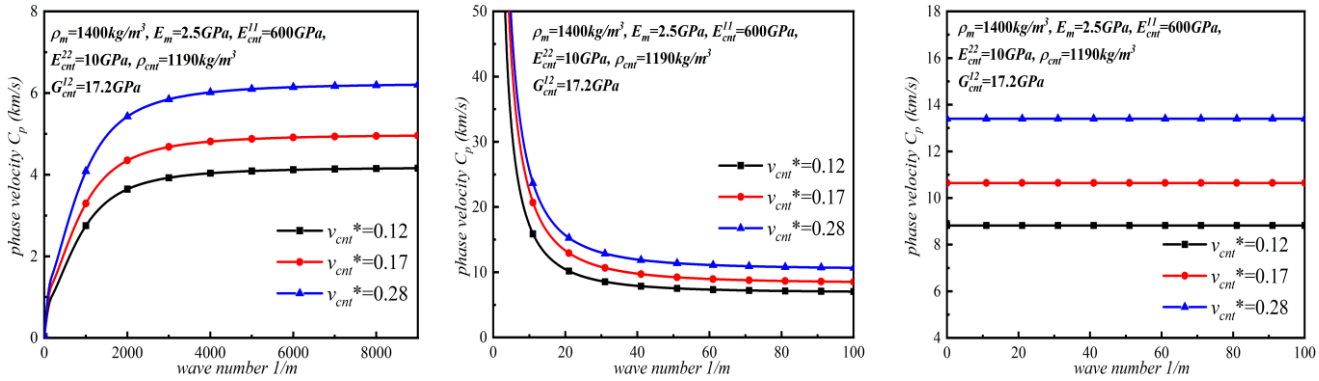

(a) (b) (c)

Fig. 4 ave propagation diagram with different volume fractions of CNTs (O-Beam)

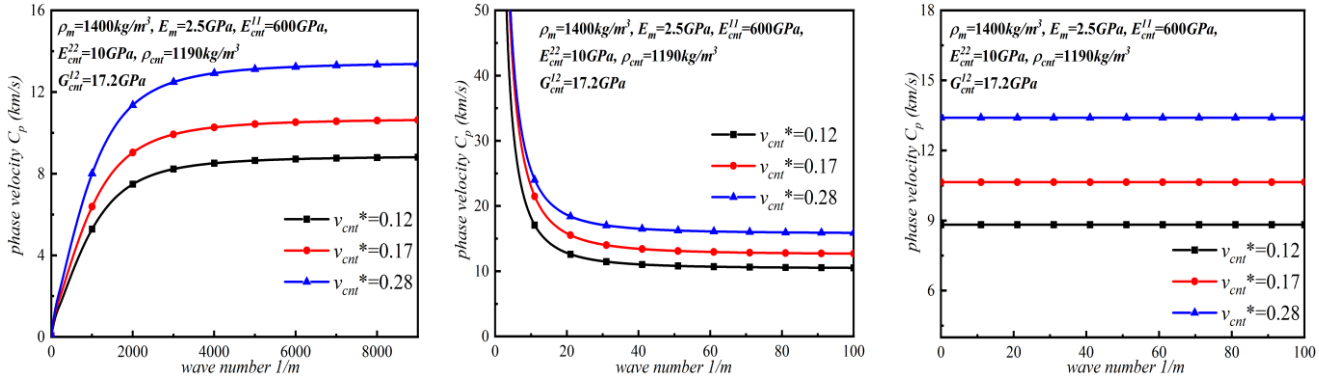

(a) (b) (c)

Fig. 5 Wave propagation diagram with different volume fractions of CNTs (X-Beam)

group velocity shows an increasing trend as the wave number increases, and when the wave number is less than 20 (1/m), the increasing trend of the group velocity of the three beams is dramatic for the same volume fraction of CNTs, and compared Fig. (6(b)) with Fig. (7(b)), it can be clearly seen that when the CNTs volume fraction is 0.28, the increasing trend of the UD-beam beam is the most dramatic and the O-beam is the smallest.

When the wave number k is greater than 20 (1/m), the growth trend of the shear wave group velocity for the three different distribution types of beams slows down and gradually converges to a certain value. When the wave number k is constant, the shear wave group velocity increases with the increase of volume fraction of CNTs for the three different distribution types of CNTRCs beams.

As far as the bending waves, it can be seen from picture (a) that despite the different enhancement patterns of CNTs, the trend of the bending wave group velocity under the influence of the wave number k is basically the same when the wave number k is less than 1000 (1/m), the bending

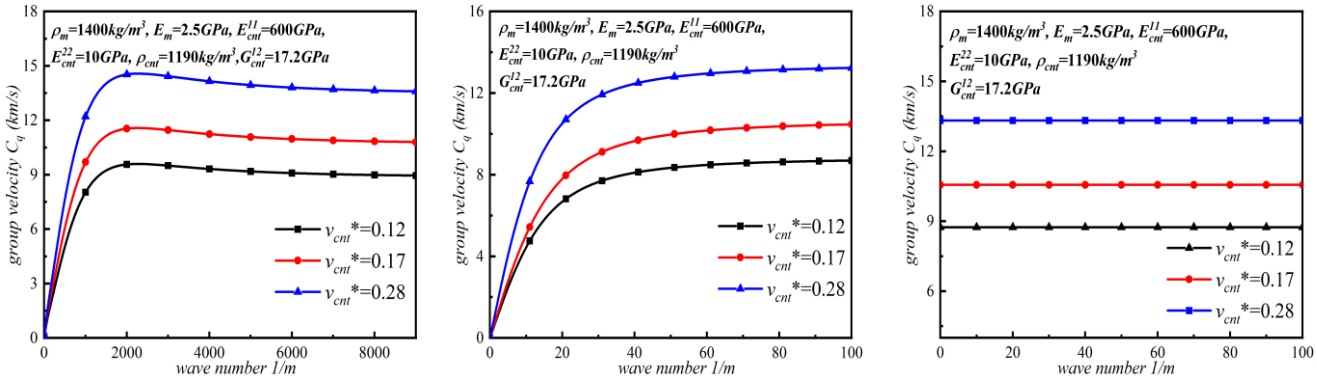

Fig. 6 Wave propagation diagram with different volume fractions of CNTs (UD-Beam)

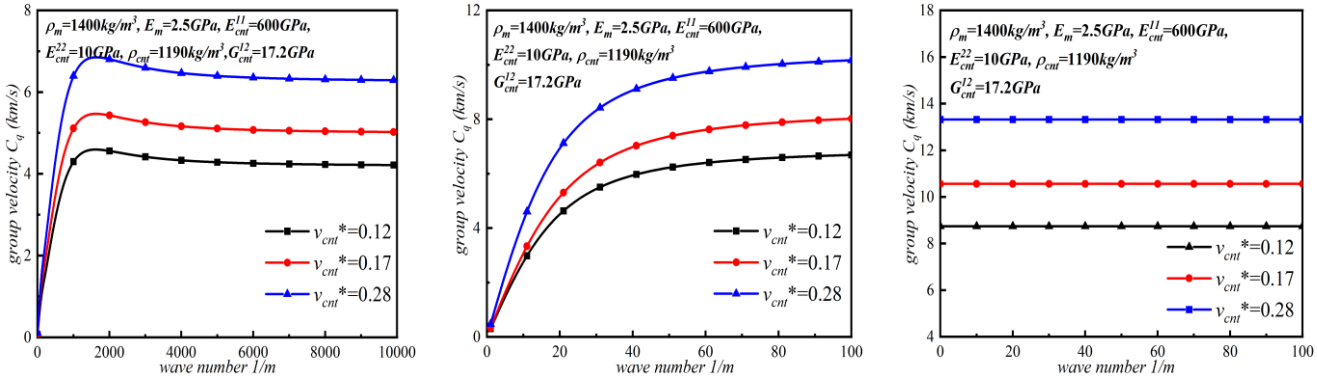

Fig. 7 Wave propagation diagram with different volume fractions of CNTs (O-Beam)

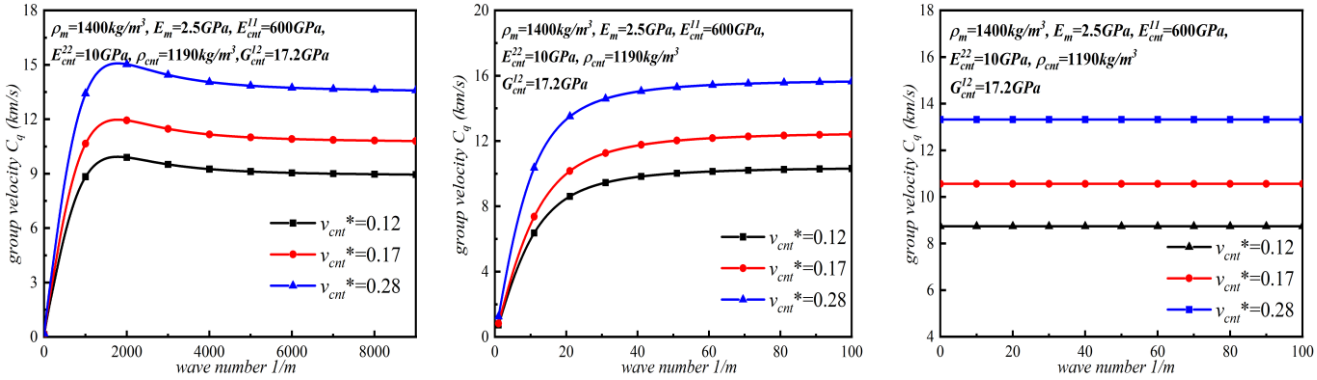

Fig. 8 Wave propagation diagram with different volume fractions of CNTs (X-Beam)

wave group velocity increases substantially with the increase of the wave number, until a maximum group velocity value occurs between the wave number of 1000 (1/m) and 2000 (1/m), and then slowly decreases to a stable value. It can be clearly observed from picture (a) of Fig. (6) to Fig. (8) that although the three different distribution types of beams bending wave group velocities follow essentially the same trend, their maximum values are quite different, with UD-beam having the largest bending wave group velocity, X-beam the next largest and O-beam the smallest. As the longitudinal group velocity of shear wave, for a specific wave number k, the larger the volume fraction of CNTs, the greater the group velocity.

In Fig. 9, we analyze the effect of spring coefficients on the bending wave phase-velocity-wave number curves for different types of beams. Taking the UD-Beam as an example, it can be seen that when the CNTs beam is placed on a Pasternak elastic base, including shear layers and Winkler springs, the phase velocity curve of bending wave of UD beam changes significantly when the elastic coefficient is zero. In contrast to the previous growth trend, the UD-Beam bending wave-phase velocity decreases

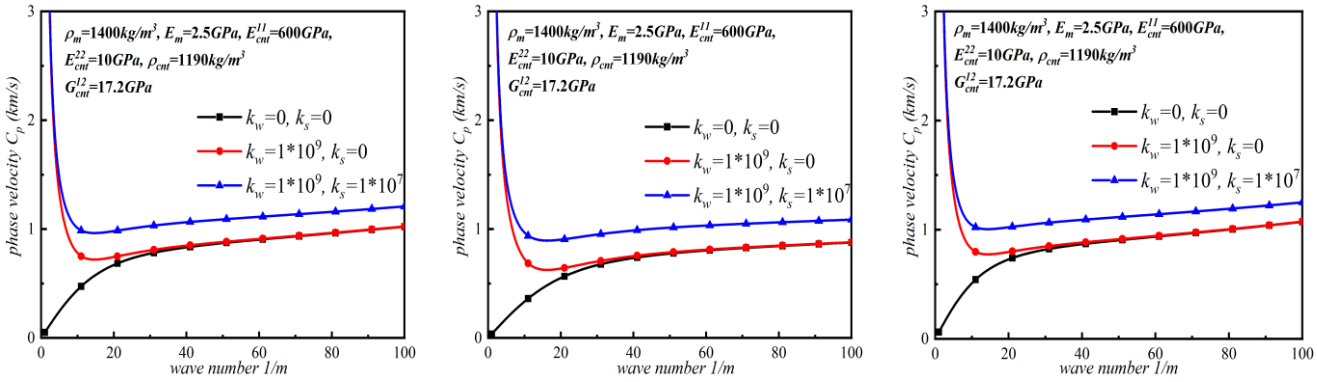

Fig. 9 Phase velocity-wave number curve of different beams types with various spring (a) UD-Beam (b) O-Beam (c) X-Beam

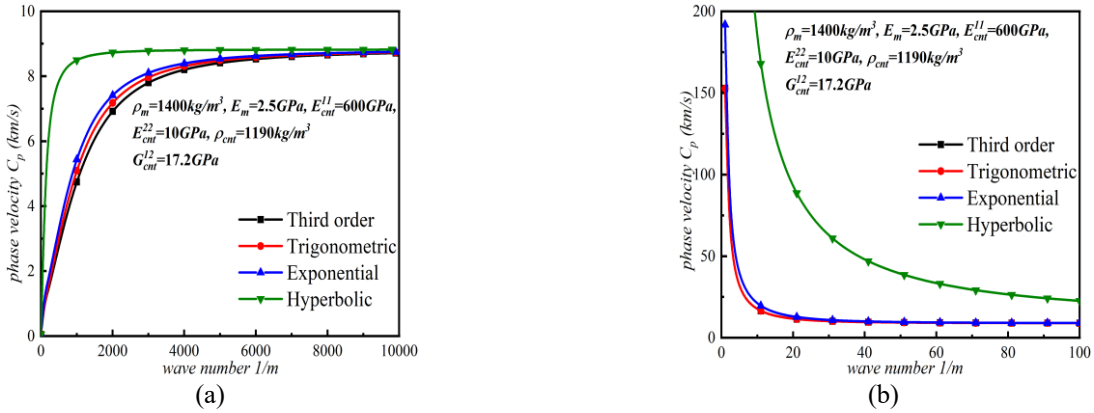

Fig. 10 Phase velocity-wave number curve with different beam theory (UD-Beam)

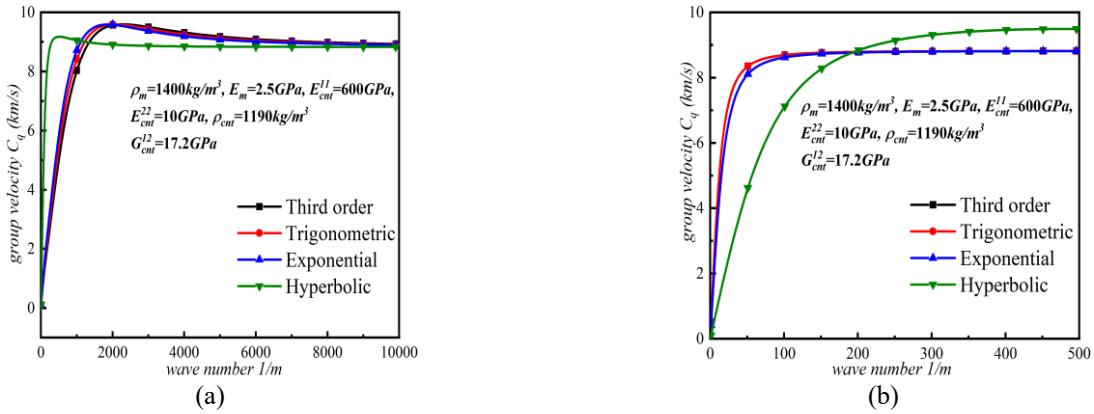

Fig. 11 Group velocity-wave number curve with different beam theory (UD-Beam)

sharply as the wave number increases, and as the wave number continues to increase, the value of the bending wave phase velocity gradually stabilizes. In addition, the author has separately investigated the effect of each of the shear layer springs and the Winkler spring on the bending phase velocity-wave number curves. The curves in Fig. 9 show that the Winkler spring has the greatest influence on the bending phase velocity, followed by the shear layer spring. Since UD-beam, X-beam and O-beam are all beams with CNTs uniformly distributed on the polymer matrix, the spring coefficient has basically the same effect on thesethree different distribution types, so the wave number curve will not be repeated.

As can be seen in (a) of Fig. 10, the bending wave phase velocity of the CNTRCs beams increases with the increasing of wave number based on different higher-order beam theory models. For Trigonometric and exponential beam theories, both of them have basically the same influence on the curve of phase velocity wave number of bending wave, and the difference between them and the

curve of phase velocity wave value under the action of Reddy's higher-order beam theory is small. On the contrary, the use of hyperbolic beam theory leads to a sharp increase in the phase velocity of bending wave when compared with the wavelet number, and the curve change trend is more obvious. In (b) of Fig. 10 depicts the phase velocity-wave number curves of shear waves under different beam theories. The phase velocity curves tend to decrease as the wave number increases, and it can be seen from the images that, similar to (a), the Hyperbolic beam theory has a more pronounced effect on the phase velocity-wave number curves.

As can be seen from (a) and (b) of Fig. 11, the different Hyperbolic beam theories can have some effect on the group velocities of the different waveforms, but in general they do not change the trend. The group velocities of the bending and shear waves still increase with the number of waves and tend to a certain value at higher wave numbers.

It can also be seen that the Hyperbolic higher order shear beam theory has a greater effect on the group velocity. The Exponential beam theory and the Trigonometric beam theory are not very different from the Reddy beam theory used in this paper.

5. Conclusions

Based on the Reddy beam model, longitudinal waves, shear waves and bending waves in CNTs beams are systematically studied. By solving an eigenvalue problem, the relation between wave number and circular frequency is obtained, and thus the relation between wave number and phase velocity, wave number and group velocity is obtained. The effects of volume fraction of CNTs, different distribution types of CNTs and elastic coefficients on the wave propagation are analyzed. Through numerical analysis, we found that:

1) The Longitudinal wave group velocity of the CNTRC beam is a constant, which is independent of the elastic coefficients and increases with the increase of the volume fractions of the CNTs.

2) The phase velocity group of shear wave decreases with the increase of wave number, and the group velocity increases with the increase of wave number. When the wave number is greater than 20, the curve gradually flattens. Under the same wave number, the CNTs increase with the increase of volume fraction.

3) As for the bending wave of CNTRC beams, the phase velocity group velocity increases with the increase of wave number under the same volume fractions of CNTs. When the wave number is very large, the curve tends to be flat.

4) It is found that when the wave number is small, the elastic coefficient has a great effect on the trend of phase velocity, but when the wave number is large, it has almost no effect.

5) It is further observed that when the wave number is small, an increase in wave number has the greatest effect on the phase velocity of the X-beam, followed by the UD-beam and O-beam.

References

Alazwari, M.A., Daikh, A.A., Houari, M.S., Tounsi, A. and Eltaher, M.A. (2021), "On static buckling of multilayered carbon nanotubes reinforced composite nanobeams supported on non-linear elastic foundations", *Steel Compos. Struct.*, **40**(3), 389-404. https://doi.org/10.12989/scs.2021.40.3.389.

Assie, A.E., Mohamed, S.A., Shanab, R.A., Abo-bakr, R.M. and Eltaher, M.A. (2023), "Static buckling of 2D FG porous plates resting on elastic foundation based on unified shear theories", *J. Appl. Comput. Mech.*, **9**(1), 239-258. https://doi.org/10.22055/jacm.2022.41265.3723.

Babaei, H. (2022a), "Nonlinear analysis of size-dependent frequencies in porous FG curved nanotubes based on nonlocal strain gradient theory", *Eng. Struct.*, 38(3), 1717-1734. https://doi.org/10.1007/s00366-021-01317-7.

Babaei, H. (2022b), "Free vibration and snap-through instability of FG-CNTRC shallow arches supported on nonlinear elastic foundation", *Appl. Math. Comput.*, **413**, 126606. https://doi.org/10.1016/j.amc.2021.126606.

Babaei, H. and Eslami, M.R. (2021a), "Nonlinear analysis of thermal-mechanical coupling bending of FGP infinite length cylindrical panels based on PNS and NSGT", *Appl. Math. Model.*, **91**, 1061-1080. https://doi.org/10.1016/j.apm.2020.10.004.

Babaei, H. and Eslami, M.R. (2021b), "Nonlinear analysis of thermal-mechanical coupling bending of clamped FG porous curved micro-tubes", *J. Therm. Stresses*, **44**(4), 409-432. https://doi.org/10.1080/01495739.2020.1870417.

Barretta, R., Ali Faghidian, S. and Marotti de Sciarra, F., Penna, R. and Pinnola F.P. (2020), "On torsion of nonlocal Lam strain gradient FG elastic beams", *Compos. Struct.*, **233**, 111550. https://doi.org/10.1016/j.compstruct.2019.111550

Basha, M., Daikh, A.A., Melaibari, A., Wagih, A., Othman, R., Almitani, K.H., Hamed, M.A., Abdelrahman, A. and Eltaher, M.A. (2022), "Nonlocal strain gradient theory for buckling and bending of FG-GRNC laminated sandwich plates", *Steel Compos. Struct.*, **43**(5), 639-660. https://doi.org/10.12989/scs.2022.43.5.639

Bensattalah, T., Hamidi, A., Bouakkaz, K., Zidour, M. and Daouadji, T.H. (2020), "Critical buckling load of triple-walled carbon nanotube based on nonlocal elasticity theory", *J. Nano Res.*, **62**, 108-119. https://doi.org/10.4028/www.scientific.net/jnanor.62.108.

Chen, X., Zhao, J.L., She, G.L., Jing, Y., Luo, J. and Pu, H.Y. (2022a), "On wave propagation of functionally graded CNT strengthened fluid-conveying pipe in thermal environment", *Eur. Phys. J. Plus.*, **137**(10), 1158. https://doi.org/10.1140/epjp/s13360-022-03234-0.

Chen, X., Zhao, J.L., She, G.L., Jing, Y., Pu, H.Y. and Luo, J. (2022b), "Nonlinear free vibration analysis of functionally graded carbon nanotube reinforced fluid-conveying pipe in thermal environment", *Steel Compos. Struct.*, **45**(5), 641-652. https://doi.org/10.12989/scs.2022.45.5.641.

Civalek, O., Akba, E.D., Akgz, B. and Dastjerdi, S. (2021a), "Forced vibration analysis of composite beams reinforced by carbon nanotubes", *Nanomaterials*, **11**(3), 571. https://doi.org/10.3390/nano11030571.

Civalek, O., Dastjerdi, S., Akbaş, S.D. and Akgöz, B. (2021b), "Vibration Analysis of Carbon Nanotube-Reinforced Composite Microbeams", *Math. Method. Appl. Sci.*, https://doi.org/10.1002/mma.7069.

Daikh, A.A., Houari, M.S.A., Karami, B., Eltaher, M.A., Dimitri, R. and Tornabene, F. (2021), "Buckling analysis of CNTRC curved sandwich nanobeams in thermal environment", *Appl. Sci.*, **11**(7), 3250. https://doi.org/10.3390/app11073250.

Ding, H.X. and She, G.L. (2021), "A higher-order beam model for the snap-buckling analysis of FG pipes conveying fluid", *Struct.*

Eng. Mech., **80**(1), 63-72. http://dx.doi.org/10.12989/sem.2021.80.1.063.

Ding, H.X., She, G.L. and Zhang, Y.W. (2022a), "Nonlinear buckling and resonances of functionally graded fluid-conveying pipes with initial geometric imperfection", *Eur. Phys. J. Plus*, **137**, 1329. https://doi.org/10.1140/epjp/s13360-022-03570-1.

Ding, H.X., Zhang, Y.W. and She, G.L. (2022b), "On the resonance problems in FG-GPLRC beams with different boundary conditions resting on elastic foundations", *Comput. Concrete*, **30**(6), 433-443. https://doi.org/10.12989/cac.2022.30.6.433.

Ding, H.X. and She, G.L. (2023), "Nonlinear resonance of axially moving graphene platelet reinforced metal foam cylindrical shells with geometric imperfection", *Archiv. Civil Mech. Eng.*, https://doi.org/10.1007/s43452-023-00634-6.

Ebrahimi, F. and Farazmandnia, N. (2018), "Vibration analysis of functionally graded carbon nanotube-reinforced composite sandwich beams in thermal environment", *Adv. Aircraft Spacecraft Sci.*, **5**(1), 107-128. https://doi.org/10.12989/aas.2018.5.1.107.

Emam, S.A., Eltaher, M.A., Khater, M.E. and Abdalla, W.S. (2018), "Postbuckling and free vibration of multilayer imperfect nanobeams under a pre-stress load", *Appl. Sci.*, **8**(11), 2238. https://doi.org/10.3390/app8112238.

Esen, I., Daikh, A.A. and Eltaher, M.A. (2022b), "Dynamic response of nonlocal strain gradient FG nanobeam reinforced by carbon nanotubes under moving point load", *Eur. Phys. J. Plus*, **136**(4),1-22. https://doi.org/10.1140/epjp/s13360-021-01419-7.

Faghidian, S.A. and Elishakoff, I. (2022a), "Wave propagation in Timoshenko-ehrenfest nanobeam: A mixture unified gradient theory", *J. Vib. Acoust.-T. ASME.*, **144**(6), 061005. https://doi.org/10.1115/1.4055805.

Faghidian, S.A., Zur, K.K., Reddy, J.N. and Ferreira, A.J.M. (2022b), "On the wave dispersion in functionally graded porous Timoshenko-Ehrenfest nanobeams based on the higher-order nonlocal gradient elasticity", *Compos. Struct.*, **279**, 114819. https://doi.org/10.1016/j.compstruct.2021.114819.

Faghidian, S.A., Zur, K.K., Pan, E. and Kim, J. (2022c), "On the analytical and meshless numerical approaches to mixture stress gradient functionally graded nano-bar in tension", *Eng. Anal. with Bound. Elem.*, **134**, 571-580. https://doi.org/10.1016/j.enganabound.2021.11.010.

Faghidian, S.A. and Elishakoff, I. (2023a), "The tale of shear coefficients in Timoshenko-Ehrenfest beam theory: 130 years of progress", *Meccanica.*, **58**(1), 97-108. https://doi.org/10.1007/s11012-022-01618-1.

Faghidian, S.A., Zur, K.K. and Pan, E.R. (2023b), "Stationary variational principle of mixture unified gradient elasticity", *Int. J. Eng. Sci.*, **182**, 103786. https://doi.org/10.1016/j.ijengsci.2022.103786.

Faghidian, S.A., Zur, K.K. and Elishakoff, I. (2023c), "Nonlinear flexure mechanics of mixture unified gradient nanobeams", *Commun. Nonlinear Sci. Numer. Simul.*, **117**, 106928. https://doi.org/10.1016/j.cnsns.2022.106928.

Gan, L.L. and She, G.L. (2023), "Nonlinear snap-buckling and resonance of FG-GPLRC curved beams with different boundary conditions", *Geomech. Eng.*, **32**(5), 541-551. https://doi.org/10.12989/gae.2023.32.5.541.

Gan, L.L., Xu, J.Q., and She, G.L. (2023), "Wave propagation of graphene platelets reinforced metal foams circular plates", Structural Engineering and Mechanics, 85(5), 645-654. https://doi.org/10.12989/sem.2023.85.5.645.

Golmakani, M.E.，Malikan, M. and Pour, S.G. (2021), "Bending analysis of functionally graded nanoplates based on a higher-order shear deformation theory using dynamic relaxation method", *Continuum Mech. Thermodynam.*, https://doi.org/10.1007/s00161-021-00995-4

Hadji, L., Meziane, M. and Safa, A. (2018), "A new quasi-3d higher shear deformation theory for vibration of functionally graded carbon nanotube-reinforced composite beams resting on elastic foundation", *Struct. Eng. Mech.*, **66**(6), 771-781. https://doi.org/10.12989/sem.2018.66.6.771.

Hendi, A., Eltaher, M.A., Mohamed, S.A. and Attia, M. (2022), "Nonlinear thermal vibration of pre/post-buckled two-dimensional FGM tapered microbeams based on a higher order shear deformation theory", *Steel Compos. Struct.*, **41**(6), 787-802. https://doi.org/10.12989/scs.2021.41.6.787.

Heydari, A. (2018), "Exact vibration and buckling analyses ofarbitrary gradation of nano-higher order rectangular beam", *Steel Compos. Struct.*, **28**(5), 589-606. https://doi.org/10.12989/scs.2018.28.5.589.

Karamanli, A. and Vo, T.P. (2021), "Finite element model for carbon nanotube-reinforced and graphene nanoplatelet-reinforced composite beams", *Compos. Struct.*, **264**, 113739. https://doi.org/10.1016/j.compstruct.2021.113739.

Khelifa, Z., Hadji, L., Daouadji, T.H. and Bourada, M. (2018), "Buckling response with stretching effect of carbon nanotube-reinforced composite beams resting on elastic foundation", *Struct. Eng. Mech.*, **67**(2), 125-130. https://doi.org/10.12989/sem.2018.67.2.125.

Ke, L.L., Yang, J. and Kitipornchai, S. (2010), "Nonlinear free vibration of functionally graded carbon nanotube-reinforced composite beams", *Compos. Struct.*, **92**(3), 676-683. https://doi.org/10.1016/j.compstruct.2009.09.024.

Li, Y.P., She, G.L., Gan, L.L. and Liu, H.B. (2023), "Nonlinear thermal post-buckling analysis of graphene platelets reinforced metal foams plates with initial geometrical imperfection", *Steel. Compos. Struct.*, **46**(5), 649-658. https://doi.org/10.12989/scs.2023.46.5.649.

Lu, L., She, G.L. and Guo, X. (2021), "Size-dependent postbuckling analysis of graphene reinforced composite microtubes with geometrical imperfection", *Int. J. Mech. Sci.*, **199**, 106428. https://doi.org/10.1016/j.ijmecsci.2021.106428.

Malikan, M. and Eremeyev, V.A. (2021), "Effect of surface on the flexomagnetic response of ferroic composite nanostructures; nonlinear bending analysis", *Compos. Struct.*, **271**, 114179. https://doi.org/10.1016/j.compstruct.2021.114179.

Mohamed, N., Mohamed, S.A. and Eltaher, M.A. (2021), "Buckling and post-buckling behaviors of higher order carbon nanotubes using energy-equivalent model", *Eng. with Comput.*, **37**(4), 2823-2836. https://doi.org/10.1007/s00366-020-00976-2.

Mohamed, N., Eltaher, M.A., Mohamed, S.A. and Seddek, L.F. (2019), "Energy equivalent model in analysis of postbuckling of imperfect carbon nanotubes resting on nonlinear elastic foundation", *Struct. Eng. Mech.*, **70**(6), 737-750. https://doi.org/10.12989/sem.2019.70.6.737.

Melaibari, A., Mohamed, S.A., Assie, A.E., Shanab, R.A. and Eltaher, M.A. (2023), "Static response of 2D FG porous plates resting on elastic foundation using midplane and neutral surfaces with movable constraints", *Mathematics*, **10**(24), 4784. https://doi.org/10.3390/math10244784.

Peng, X.B., Xu, J., Yang, E.C., Li, Y.H. and Yang, J. (2022), "Influence of the boundary relaxation on free vibration of functionally graded carbon nanotube-reinforced composite beams with geometric imperfections", *Acta Mechanica*, **233**, 4161-4177. https://doi.org/10.1007/s00707-022-03320-5.

Rafiee, M., Jie, Y. and Kitipornchai, S. (2013), "Large amplitude vibration of carbon nanotube reinforced functionally graded composite beams with piezoelectric layers", *Compos. Struct.*, **96**, 716-725. https://doi.org/10.1016/j.compstruct.2012.10.005.

Selmi, A. (2021), "Nonlinear behavior of single walled carbon nanotube reinforced aluminium alloy beam", *J. Nano Res.*, **69**, 89-103. https://doi.org/10.4028/www.scientific.net/JNanoR.69.89.

She, G.L. (2020), "Wave propagation of FG polymer composite nanoplates reinforced with GNPs", *Steel Compos. Struct*., **37**(1), 27-35. https://doi.org/10.12989/scs.2020.37.1.027.

She, G.L. (2021), "Guided wave propagation of porous functionally graded plates: The effect of thermal loadings", *J. Therm. Stresses*., **44**(10), 1289-1305. https://doi.org/10.1080/01495739.2021.1974323

She, G.L. and Ding, H.X. (2023), "Nonlinear primary resonance analysis of initially stressed graphene platelet reinforced metal foams doubly curved shells with geometric imperfection", *Acta Mech. Sin*., **39**, 522392. https://doi.org/10.1007/s10409-022-22392-x.

She, G.L., Ding, H.X. and Zhang, Y.W. (2022), "Wave propagation in a FG circular plate via the physical neutral surface concept", *Struct. Eng. Mech*., **82**(2), 225-232. https://doi.org/10.12989/sem.2022.82.2.225.

She, G.L. and Li, Y.P. (2022), "Wave propagation in an FG circular plate in thermal environment", *Geomech. Eng*., **31**(6), 615-622. https://doi.org/10.12989/gae.2022.31.6.615.

She, G.L., Liu, H.B. and Karami, B. (2021), "Resonance analysis of composite curved microbeams reinforced with graphene nanoplatelets", *Thin Wall. Struct*., **160**, 107407. https://doi.org/10.1016/j.tws.2020.107407.

She, G.L., Yan, K.M., Zhang, Y.L., Liu, H.B. and Ren, Y.R. (2018). "Wave propagation of functionally graded porous nanobeams based on non-local strain gradient theory", *Eur. Phys. J. Plus*., **133**(9), 368. https://doi.org/10.1140/epjp/i2018-12196-5.

Shenas, A.G., Malekzadeh, P. and Ziaee, S. (2017), "Vibration analysis of pre-twisted functionally graded carbon nanotube reinforced composite beams in thermal environment", *Compos. Struct*., **162**, 325-340. https://doi.org/10.1016/j.compstruct.2018.03.104

Talebizadehsardari, P., Eyvazian, A., and Mahani, R.B. (2020), "Static bending analysis of functionally graded polymer composite curved beams reinforced with carbon nanotubes", Thin-walled structures, 157, 107139. http://dx.doi.org/10.1016/j.tws.2020.107139

Tayeb, B., Mohamed, Z., Tahar, H.D. and Khaled, B. (2019), "Theoretical analysis of chirality and scale effects on critical buckling load of zigzag triple walled carbon nanotubes under axial compression embedded in polymeric matrix", *Struct. Eng. Mech*., **70**(3), 269-277. https://doi.org/10.12989/sem.2019.70.3.269.

Timesli, A. (2020), "Buckling analysis of double walled carbon nanotubes embedded in Kerr elastic medium under axial compression using the nonlocal Donnell shell theory", *Adv. Nano. Res*., **9**(2), 69-82. https://doi.org/110.12989/anr.2020.9.2.069.

Wattanasakulpong, N. and Ungbhakorn, V. (2013), "Analytical solutions for bending, buckling and vibration responses of carbon nanotube-reinforced composite beams resting on elastic foundation", *Comput. Mater. Sci*., **71**, 201-208. https://doi.org/10.1016/j.commatsci.2013.01.028.

Xu, J.Q. and She, G.L. (2022), "Thermal post-buckling analysis of porous functionally graded pipes with initial geometric imperfection", *Geomech. Eng*., **31**(3), 329-337. https://doi.org/10.12989/gae.2022.31.3.329.

Zhang, Y.W., Ding, H.X. and She, G.L. (2022), "Snap-buckling and resonance of functionally graded graphene reinforced composites curved beams resting on elastic foundations in thermal environment", *J. Therm. Stresses*, **45**(12), 1029-1042. https://doi.org/10.1080/01495739.2022.2125137.

Zhang, Y.W., Ding, H.X. and She, G.L. (2023a), "Wave propagation in spherical and cylindrical panels reinforced with carbon nanotubes", *Steel Compos. Struct*., **46**(1), 133-141. https://doi.org/10.12989/scs.2023.46.1.133.

Zhang, Y.W., She, G.L. and Ding, H.X. (2023b), "Nonlinear resonance of graphene platelets reinforced metal foams plates under axial motion with geometric imperfections", *Eur. J. Mech. A-Solid.*, **98**, 104887. https://doi.org/10.1016/j.euromechsol.2022.104887.

Zhang, Y.W., She, G.L., Gan, L.L. and Li, Y.P. (2023c), "Thermal post-buckling behavior of GPLRMF cylindrical shells with initial geometrical imperfection", *Geomech. Eng*., **32**(6), 615-625. https://doi.org/10.12989/gae.2023.32.6.615.

Zhang, Y.W. and She, G.L. (2022), "Wave propagation and vibration of FG pipes conveying hot fluid", *Steel Compos, Struct*., **42**(3) 397-405. https://doi.org/10.12989/scs.2022.42.3.397.

Zhang, Y.W. and She, G.L. (2023a), "Nonlinear low-velocity impact response of graphene platelet-reinforced metal foam cylindrical shells under axial motion with geometrical imperfection", *Nonlinear Dynam*., **111**, 6317-6334 https://doi.org/10.1007/s11071-022-08186-9.

Zhang, Y.W. and She, G.L. (2023b), "Nonlinear primary resonance of axially moving functionally graded cylindrical shells in thermal environment", *Mech. Adv. Mater. Struct*., https://doi.org/10.1080/15376494.2023.2180556.

Zhang, Y.Y., Wang, X.Y., Zhang, X., Shen, H.M. and She, G.L. (2021), "On snap-buckling of FG-CNTRC curved nanobeams considering surface effects", *Steel Compos. Struct*., **38**(3), 293-304. https://doi.org/10.12989/scs.2021.38.3.293.

Zhao, J.L., Chen, X., She, G.L., Jing, Y., Bai, R.Q., Yi, J., Pu, H.Y. and Luo, J. (2022a), "Vibration characteristics of functionally graded carbon nanotube-reinforced composite double-beams in thermal environments", *Steel Compos. Struct*., **43**(6), 797-808. https://doi.org/10.12989/scs.2022.43.6.797.

Zhao, J.L., She, G.L., Wu, F., Yuan, S.J., Bai, R.Q., Pu, H.Y., Wang, S.L. and Luo, J. (2022b), "Guided waves of porous FG nanoplates with four edges clamped", *Adv. Nano. Res*., **13**(5), 465-474. https://doi.org/10.12989/anr.2022.13.5.465.

Zouatnia, N., Hadji, L. and Kassoul, A. (2017), "A refined hyperbolic shear deformation theory for bending of functionally graded beams based on neutral surface position", *Struct. Eng. Sci*., **63**(5), 683-689. http://doi.org/10.12989/sem.2017.63.5.683.

Zenkour, A.M. (2018), "A quasi-3D refined theory for functionally graded single-layered and sandwich plates with porosities", *Compos. Struct*., **201**, 38-48. https://doi.org/10.1016/j.compstruct.2018.05.147.

Zenkour, A.M. and Radwan, A.F. (2019), "Bending response of FG plates resting on elastic foundations in hygro thermal environment with porosities", *Compos. Struct*., **213**, 133-143. https://doi.org/10.1016/j.compstruct.2019.01.065.

CC